doi:10.1093/brain/awx273 BRAIN 2017: 140; 3112–3127 | 3112

BRAIN
A JOURNAL OF NEUROLOGY

CLINICAL TRIAL

Hereditary spastic paraplegia type 5: natural history, biomarkers and a randomized controlled trial

Ludger Schöls,[1,2,*] Tim W. Rattay,[1,2,*] Peter Martus,[3] Christoph Meisner,[3] Jonathan Baets,[4,5,6] Imma Fischer,[3] Christine Jägle,[7] Matthew J. Fraidakis,[8] Andrea Martinuzzi,[9] Jonas Alex Saute,[10,11,12] Marina Scarlato,[13] Antonella Antenora,[14] Claudia Stendel,[15,16,17] Philip Höflinger,[1,2] Charles Marques Lourenco,[18,19] Lisa Abreu,[20,21] Katrien Smets,[4,5,6] Martin Paucar,[22] Tine Deconinck,[4,6] Dana M. Bis,[20,21] Sarah Wiethoff,[1,2,23] Peter Bauer,[24,25] Alessia Arnoldi,[26] Wilson Marques,[18] Laura Bannach Jardim,[10,11,12,19] Stefan Hauser,[1,2] Chiara Criscuolo,[14] Alessandro Filla,[14] Stephan Züchner,[20,21] Maria Teresa Bassi,[26] Thomas Klopstock,[15,16,17] Peter De Jonghe,[4,5,6] Ingemar Björkhem[27] and Rebecca Schüle[1,2]

*These authors contributed equally to this work.

Spastic paraplegia type 5 (SPG5) is a rare subtype of hereditary spastic paraplegia, a highly heterogeneous group of neurodegenerative disorders defined by progressive neurodegeneration of the corticospinal tract motor neurons. SPG5 is caused by recessive mutations in the gene *CYP7B1* encoding oxysterol-7α-hydroxylase. This enzyme is involved in the degradation of cholesterol into primary bile acids. CYP7B1 deficiency has been shown to lead to accumulation of neurotoxic oxysterols. In this multicentre study, we have performed detailed clinical and biochemical analysis in 34 genetically confirmed SPG5 cases from 28 families, studied dose-dependent neurotoxicity of oxysterols in human cortical neurons and performed a randomized placebo-controlled double blind interventional trial targeting oxysterol accumulation in serum of SPG5 patients. Clinically, SPG5 manifested in childhood or adolescence (median 13 years). Gait ataxia was a common feature. SPG5 patients lost the ability to walk independently after a median disease duration of 23 years and became wheelchair dependent after a median 33 years. The overall cross-sectional progression rate of 0.56 points on the Spastic Paraplegia Rating Scale per year was slightly lower than the longitudinal progression rate of 0.80 points per year. Biochemically, marked accumulation of CYP7B1 substrates including 27-hydroxycholesterol was confirmed in serum ($n = 19$) and cerebrospinal fluid ($n = 17$) of SPG5 patients. Moreover, 27-hydroxycholesterol levels in serum correlated with disease severity and disease duration. Oxysterols were found to impair metabolic activity and viability of human cortical neurons at concentrations found in SPG5 patients, indicating that elevated levels of oxysterols might be key pathogenic factors in SPG5. We thus performed a randomized placebo-controlled trial (EudraCT 2015-000978-35) with atorvastatin 40 mg/day for 9 weeks in 14 SPG5 patients with 27-hydroxycholesterol levels in serum as the primary outcome measure. Atorvastatin, but not placebo, reduced serum 27-hydroxycholesterol from 853 ng/ml [interquartile range (IQR) 683–1113] to 641 (IQR 507–694) (−31.5%, $P = 0.001$, Mann-Whitney U-test). Similarly, 25-hydroxycholesterol levels in serum were reduced. In cerebrospinal fluid 27-hydroxycholesterol was reduced by 8.4% but this did not significantly differ from placebo. As expected, no effects were seen on clinical outcome parameters in this short-term trial. In this study, we define the mutational and phenotypic spectrum of SPG5, examine the correlation of disease severity and progression with oxysterol concentrations, and demonstrate in a randomized controlled trial that atorvastatin treatment can effectively lower 27-hydroxycholesterol levels in serum of SPG5 patients. We thus demonstrate the first causal treatment strategy in hereditary spastic paraplegia.

Received May 2, 2017. Revised August 22, 2017. Accepted August 26, 2017. Advance Access publication November 6, 2017

1 Center for Neurology and Hertie Institute for Clinical Brain Research, Eberhard-Karls-University, 72076 Tübingen, Germany
2 German Center of Neurodegenerative Diseases (DZNE), 72076 Tübingen, Germany
3 Institute for Clinical Epidemiology and Applied Biostatistics, Eberhard-Karls-University, 72076 Tübingen, Germany
4 Neurogenetics Group, Center for Molecular Neurology, VIB, 2610 Antwerp, Belgium
5 Department of Neurology, Antwerp University Hospital, 2610 Antwerp, Belgium
6 Laboratory of Neuromuscular Pathology, Institute Born-Bunge, University of Antwerp, 2610 Antwerp, Belgium
7 Center for Rare Diseases and Institute of Human Genetics and Applied Genomics, Eberhard-Karls-University, 72076 Tübingen, Germany
8 Rare Neurological Diseases Unit, Department of Neurology, University Hospital 'Attikon', Medical School of the University of Athens, 12462 Athens, Greece
9 Scientific Institute IRCCS E. Medea, Conegliano Research Center, 31015 Conegliano, Italy
10 Medical Genetics Service, Hospital de Clínicas de Porto Alegre, Porto Alegre, Brazil
11 Genetics Identification Laboratory, Hospital de Clínicas de Porto Alegre, 90035 Porto Alegre, Brazil
12 Postgraduate Program in Medicine: Medical Sciences, Universidade Federal do Rio Grande do Sul (UFRGS), 90040 Porto Alegre, Brazil
13 Neurology Department and INSPE, San Raffaele Hospital, 20132 Milan, Italy
14 Department of Neurosciences, Reproductive and Odontostomatological Sciences, Federico II University Naples, 80131 Naples, Italy
15 Department of Neurology, Friedrich Baur Institute, Ludwig-Maximilians-University, 80336 Munich, Germany
16 Munich Cluster for Systems Neurology (SyNergy), 81377 Munich, Germany
17 German Center for Neurodegenerative Diseases (DZNE), 81377 Munich, Germany
18 Departamento de Neurologia, Faculdade de Medicina de Ribeirao Preto, Universidade de Sao Paulo, 14049 Ribeirao Preto, Brazil
19 Department of Internal Medicine, Universidade Federal do Rio Grande do Sul (UFRGS), 90040 Porto Alegre, Brazil
20 John P. Hussman Institute for Human Genomics, Dr. John T. Macdonald Foundation Department of Human Genetics, University of Miami, 33136 Miami, Florida, USA
21 Dr. John T. Macdonald Foundation Department of Human Genetics, University of Miami, 33136 Miami, Florida, USA
22 Department of Neurology, Karolinska University Hospital Huddinge and Department of Clinical Neuroscience, Karolinska Institute, 14152 Huddinge, Sweden
23 Institute of Neurology, Queen Square, London WC1N 3BG, UK
24 Institute of Medical Genetics and Applied Genomics, Eberhard-Karls-University, 72076 Tübingen, Germany
25 CENTOGENE AG, 18057 Rostock, Germany
26 Laboratory of Molecular Biology, Scientific Institute IRCCS E. Medea, 23842 Bosisio Parini, Italy
27 Karolinska University Hospital Huddinge, Karolinska Institute, 14152 Stockholm, Sweden

Correspondence to: Rebecca Schüle, MD,
Hertie Institute for Clinical Brain Research, Otfried-Müller-Str. 27, 72076 Tübingen, Germany
E-mail: Rebecca.Schuele-Freyer@uni-tuebingen.de

Correspondence may also be addressed to: Ludger Schöls, MD,
Center for Neurology, Hoppe-Seyler Strasse 3, 72076 Tübingen, Germany
E-mail: Ludger.Schoels@uni-tuebingen.de

Keywords: hereditary spastic paraplegia; SPG5; biomarker; randomized controlled trial; oxysterol

Abbreviations: 25/27-OHC = 25/27-hydroxycholesterol; 3β-CA = 3β-hydroxy-5-cholestenoic acid; HSP = hereditary spastic paraplegia; iPSC = induced pluripotent stem cell; SPG5 = spastic paraplegia 5; SPRS = Spastic Paraplegia Rating Scale

Introduction

Spastic paraplegia 5 (SPG5) is a rare subtype of hereditary spastic paraplegia (HSP), a group of diseases that is characterized by progressive lower limb spasticity and weakness due to degenerative axonopathy of corticospinal tract motor neurons. It is caused by bi-allelic mutations in the oxysterol-7α-hydroxylase gene *CYP7B1* (Tsaousidou *et al.*, 2008). This enzyme is involved in the degradation of cholesterol into primary bile acids. The bulk of cholesterol is degraded via the so-called 'classic' pathway that is initiated by 7α-hydroxylation of cholesterol by CYP7A1. Alternatively, cholesterol is initially side chain oxidized and the resulting oxysterols 25-hydroxycholesterol (25-OHC) and 27-hydroxycholesterol (27-OHC) are 7α-hydroxylated by CYP7B1 ('acidic' pathway) (Supplementary material and Supplementary Fig. 1). 27-OHC can be further oxidized to 3β-hydroxy-5-cholestenoic acid (3β-CA) especially under low-cholesterol conditions (Pikuleva *et al.*, 1998). CYP7B1 deficiency in SPG5 leads to marked accumulation of CYP7B1 substrates in serum and CSF (Schule *et al.*, 2010). This finding is important as it has potential therapeutic implications for SPG5. Oxysterols, especially 27-OHC, have been repeatedly linked to neurodegeneration (Lim *et al.*, 2014). They have a pro-apoptotic effect on cultured neuroblastoma cells, macrophages and smooth

muscle cells (Rantham Prabhakara *et al.*, 2008; Riendeau and Garenc, 2009). 27-OHC is pro-amyloidogenic by stimulating β-secretase activity (Famer *et al.*, 2007) and causes Alzheimer disease-like pathology in human neuroblastoma SH-SY5Y cells (Prasanthi *et al.*, 2009). The spinal cord does not express *CYP46A1*, the gene encoding the main cholesterol metabolizing enzyme in brain, and therefore might be especially prone to 27-OHC effects (Bjorkhem *et al.*, 2010). Oxysterol accumulation thus may not only be a biomarker for, but also a key factor driving pathology in SPG5 (Theofilopoulos *et al.*, 2014).

Cholesterol and oxysterol levels in serum and CSF are related (Leoni *et al.*, 2003) and cholesterol lowering therapy has been shown to reduce 27-OHC levels in plasma (Thelen *et al.*, 2006). Treatment of SPG5 patients with HMG-CoA reductase inhibitors might therefore lower the pathologically elevated levels of oxysterols in SPG5 patients (Schule *et al.*, 2010; Mignarri *et al.*, 2015).

To test this hypothesis we here report a detailed clinical and biochemical analysis of oxysterols in a large cohort of SPG5 patients, analyse the natural history of SPG5, evaluate the correlation between oxysterol levels and disease duration and severity, demonstrate toxicity of oxysterols on human cortical neurons at concentrations found in SPG5 patients and report the results of a randomized placebo-controlled double blind clinical trial to examine the efficacy of cholesterol lowering therapy with atorvastatin on oxysterol levels in SPG5.

Patients and methods

Cohort and clinical work-up

A total of 34 subjects from 28 families with a clinical diagnosis of HSP and genetically confirmed SPG5 (Schule *et al.*, 2009; Schlipf *et al.*, 2011) were recruited in clinical centres in Antwerp (Belgium), Athens (Greece), Conegliano, Lecco (Italy), Milano (Italy), Munich (Germany), Naples (Italy), Tübingen (Germany), Porto Alegre (Brazil) and Sao Paolo (Brazil). Additionally, 11 unaffected family members, carrying heterozygous *CYP7B1* mutations, were included. All probands received a detailed neurological examination by a movement disorder specialist at the respective clinical centre including application of the Spastic Paraplegia Rating Scale (SPRS) (Schule *et al.*, 2006). For cross-sectional analyses of disease severity, the first SPRS score in each proband was selected; for longitudinal analyses, all available SPRS scores were included. Phenotypes were classified into pure and complicated HSP according to the Harding criteria (Harding, 1983). Written informed consent was obtained from all study participants; the local institutional review boards approved the study.

Biochemical analysis

Serum and CSF were sampled from patients and healthy family members. Side-chain oxidized oxysterols and 3β-CA were assayed by isotope dilution mass spectrometry using deuterium-labelled internal standards as described previously (Bjorkhem and Falk, 1983; Dzeletovic *et al.*, 1995). For cross-sectional analysis, the first available values were used.

Derivation of fibroblasts

Dermal fibroblasts from a voluntary healthy donor unrelated to the study cohort (female, aged 46 years at biopsy) were cultivated as described in Hauser *et al.* (2016).

Generation of human induced pluripotent stem cells and neuronal differentiation

Induced pluripotent stem cells (iPSCs) were generated and characterized as described in Hauser *et al.* (2016) and differentiated into cortical neurons following a protocol published by Shi *et al.* (2012), with minor modifications (Supplementary material). Neural induction was initiated by addition of 3N medium (1:1 mixture of N2- and B27-containing media), supplemented with 10 µM SB431542 and 500 nM LDN-193189 (Sigma-Aldrich). Medium was changed daily. At Day 10, cells were collected by dissociation with Accutase® (Life Technologies) and replated in 3N medium supplemented with 20 ng/ml FGF2 on Matrigel®-coated well plates. At Day 12, FGF2 was withdrawn and cells were further cultivated including medium changes to 3N medium every other day (Supplementary material).

Cultivation of NSC-34 cells

Cells were plated onto 96-well plates with a cell density of 5×10^4 cells per well and cultured for 3 days in Dulbecco's modified Eagle medium (DMEM) + 1% foetal calf serum (Gibco, Thermo Fisher Scientific) supplemented with 24-OHC, 25-OHC, 27-OHC or 3β-CA at concentrations varying from 0.5 nM to 50 µM.

Cell proliferation and cytotoxicity assay

To measure metabolic activity and cytotoxicity, the colorimetric Cell Proliferation Reagent WST-1 assay and the Cytotoxicity Detection Kit LDH (Roche) were used. The absorbance of the developed dye was measured on a microplate reader at 450 nm or 490 nm, respectively with a reference wavelength of 650 nm after 2 h incubation (WST) or 1 h incubation (LDH). Substance control was 1% DMSO (27-OHC) or 1% ethanol (3β-CA) and as a positive control, cells were treated with 1% Triton™ X-100 for 30 min prior to the assay.

Neurite outgrowth

After incubation with oxysterols (50 nM, 5 days) cells were fixated and immunostained against tau (AB75714, abcam/Alexa Fluor® 488 nm secondary goat-anti chicken, A11039, dilution 1:1000, Invitrogen, Thermo Fisher Scientific) and alpha-tubulin (T6074, Sigma-Aldrich/Alexa Fluor® 568 nm secondary goat-anti mouse antibody, A11004, dilution 1:1000, Invitrogen). Images were taken on the Zeiss Axio

Imager Z.1 microscope. Total neurite length measured in µm ($n = 50$) and total number of branching points per cell ($n = 50$) were quantified using the NeuronJ plugin of the ImageJ software (http://imagej.nih.gov/ij/).

Statistical analysis: natural history and biomarker studies

Quantitative variables are reported as mean and standard deviation (SD) (normally distributed data) or median and interquartile range (IQR). To compare categorical variables across groups we used logistic regression analysis. To identify predictors for the SPRS score and oxysterol concentrations we applied linear regression. The Kaplan-Meier method was used to describe censored data (walking aid use, wheelchair use) and Cox proportional hazard analysis was applied to assess the influence of age of onset on walking aid and wheelchair use. To assess the longitudinal progression rate, we performed linear regression analysis and quantified the SPRS increase over time in each patient. The average progression rate per year was calculated from the unstandardized regression coefficient. P-values $\leqslant 0.05$ were considered statistically significant unless stated otherwise. SPSS Statistics version 21 (Chicago, IL, USA) (descriptive analysis, linear mixed and logistic model) for Windows and R release 3.2.2 (Cox model corrected for family clusters) were used for statistical calculations; JMP v11 (SAS, Cary, NC, USA) for Mac was used for graph generation.

Interventional trial

We designed a randomized placebo-controlled double-blind trial with atorvastatin (40 mg/day) for 9 weeks in adults. Children under 18 years of age received a reduced dosage of 20 mg/day.

Fourteen SPG5 patients aged 15–51 years were recruited by clinical centres of the German HSP Network in Tübingen and Munich and the neuromuscular clinic in Antwerp. All participants gave their written informed consent. Probands with clinically manifest HSP and a genetically confirmed diagnosis of SPG5 (Supplementary Table 1) older than 10 years were eligible to participate in the study. Exclusion criteria comprised treatment with statins 3 months prior to enrolment, contraindications to statin therapy according to the summary of product characteristics (hypersensitivity to atorvastatin, active liver disease), concomitant treatment with strong CYP3A4 inhibitors (e.g. amiodarone, clarithromycin, diltiacem, tamoxifen, verapamil) or fibrates within 7 days before enrolment, and an elevation of liver transaminases >3 times the upper limit of normal. Pregnancy was excluded in women of childbearing age. All probands screened for participation were eligible for the study. Randomization was carried out in blocks of four using the online tool Randomization.com.

Primary endpoint of this study was the change of 27-OHC in serum after 9 weeks. Secondary outcome measures included change of 27-OHC in CSF as well as reduction of 24-OHC, 25-OHC and 3β-CA levels in serum and CSF. Additionally, bile acids were assessed using mass spectrometry according to standard protocols (Bjorkhem and Falk, 1983; Dzeletovic *et al.*, 1995). Blood and CSF samples were taken in the morning from fasting patients. Clinical outcome measures included the change of the SPRS total score as a measure of disease severity in HSP (Schule *et al.*, 2006), the 3-min endurance walk (Crapo *et al.*, 2002; Iriberri *et al.*, 2002; Borg, 2016) and the physical cost index (PCI) (MacGregor, 1981) as a measure of physical exertion during prolonged activity.

Trial statistics

To obtain an estimate of the effect size of the treatment we treated four SPG5 patients with atorvastatin 40 mg over an 8-week period and measured oxysterol levels in serum ($n = 4$) and CSF ($n = 3$) before and after treatment (Supplementary Table 1 and Supplementary Fig. 3). All four patients responded to treatment with a decrease of serum cholesterol levels by an average of 38% (range 28–49%) from 193 mg/dl to 116 mg/dl. Serum 27-OHC, the selected primary outcome measure, decreased in all patients with an average reduction by 31% from 893 mg/dl before treatment to 617 mg/dl after treatment and dropped by 20% from 19.5 ng/ml to 15.2 ng/ml in CSF. Based on the thus determined large effect size, we assumed a small sample size and decided to use a one-sided Mann-Whitney U-test. Our power calculation determined that a sample size of six in each group had 80% power to detect a probability of 0.075 that an observation in the atorvastin group was less than an observation in the placebo group using a Mann-Whitney U-test with a 0.050 one-sided significance level (NQuery 7.0).

The statistical analyses included all randomized patients (intention-to-treat). As no major protocol violations were observed, no per-protocol analyses were performed. Data were complete for all patients, rendering missing data replacement unnecessary. The secondary outcomes were compared and statistically assessed using two-sided Mann-Whitney U-tests with explorative intention. Changes of outcome variables within groups from baseline to 9 weeks were compared and statistically assessed using sign rank tests. The demographic variables were described using frequencies for qualitative variables and median/range for quantitative variables. Mann-Whitney U-tests and Fisher's exact tests were used to compare the demographics between the two groups. SAS software, version 9.2 was used for statistical analysis; graphs were generated with JMP 11 for Mac (SAS Institute).

Study approval

The study was approved by the Medical Ethics Board of the University of Tübingen (vote 247/2015) and the national regulatory institution (Bundesamt für Arzneimittel und Medizinprodukte – BfArM) and was registered as EudraCT 2015-000978-35.

Results

Phenotypic spectrum

We collected 34 genetically confirmed SPG5 cases from 28 families, six of which have been previously published with limited clinical information (Families F1–F5; Supplementary Table 1) (Schule *et al.*, 2009, 2010). Age at onset varied considerably between ages 1 to 63 with a median age at

onset of 13 years (IQR 6–33). Although SPG5 would be classified as 'pure' HSP according to the Harding criteria (Harding, 1983), in most of our cases (26/34, 76%), there were several discriminating features even in the so-called pure cases. Dorsal column sensory deficits were unusually severe compared to other types of HSP (Schule *et al.*, 2016), often presenting as loss of vibration sense and deficits of joint position sense of the lower extremities. Consequently, a high percentage of SPG5 patients had afferent gait ataxia and/or lower limb ataxia (16/34, 47%). Urge incontinence or voiding affected 55% of SPG5 patients; additionally, 15% of SPG5 patients reported rectal urge symptoms and faecal incontinence. Behavioural abnormalities including panic disorder, substance abuse and attention deficit hyperactivity disorder (ADHD) were observed in three cases. Other co-morbidities included developmental dysplasia of the hip ($n = 4$), cluster headache ($n = 1$), early ovarian failure ($n = 1$), and grand mal seizures ($n = 1$) (Table 1 and Supplementary Table 1).

Mutation spectrum of SPG5

Among the 24 different mutations we identified in the 28 families included in this study, 11 mutations were novel (Supplementary Table 2). As loss-of-function is the established disease mechanism in SPG5 (Schule *et al.*, 2010), we assumed all novel truncating mutations to be pathogenic ($n = 5$). The remaining six novel missense variants affected without exception highly conserved amino acid residues, were predicted to be pathogenic by several *in silico* prediction algorithms and absent from public databases (dbSNP, Exome Variant Server EVS, Exome Aggregation Consortium Browser ExAC) (Supplementary Table 3). Variants were confirmed to segregate following an autosomal-recessive inheritance pattern in all families.

Truncating mutations are associated with an earlier age at onset

In our cohort, 16 cases carried solely missense mutations and 18 cases carried at least one truncating mutation of the *CYP7B1* gene. Presence of truncating mutations advanced disease onset by two decades (Fig. 1A).

Natural history

Clinical measures of disease progression

SPRS, timed walking tests and walking aid dependency

Little is known about disease progression in SPG5. Median disease severity on the SPRS was 22 points (available for 31 cases, IQR 12–29) after a median disease duration of 13 years (IQR 9–28). The cross-sectional progression rate, obtained by dividing the SPRS score by the disease duration in each individual, was 0.56 SPRS points per year (Fig. 1B).

To analyse the time from symptom onset to walking aid and wheelchair dependency in SPG5 we performed a Kaplan-Meier analysis. Data were available for 23 SPG5 patients, 11 of whom were walking aid-dependent and six of whom were wheelchair-dependent at the end of the study. Median disease duration until walking aid dependency was 23 years (IQR 12–33) and median age at walking aid dependency was 37 years (IQR 28–43 years) (Fig. 1E). Later age of onset and higher SPRS scores were associated with a higher risk to become walking aid-dependent [age of onset: $B = 0.14$, 95% confidence interval (CI) 0.05–0.28, $P = 0.0027$; SPRS: $B = 0.12$, 95% CI 0.03–0.23, $P = 0.0092$]. Wheelchair dependency occurred in SPG5 after a median disease duration of 33 years (Fig. 1F) (for more details and discussion see Supplementary material).

In patients who were still able to walk a 10 m distance and/or climb 10 steps, the time needed to perform these tasks (item 3/item 5 of the SPRS) was a good predictor

Table 1 Clinical and neurophysiological summary characteristics of the SPG5 cohort

Number of patients/ families	34 affected/ 28 families
Gender	16 male / 18 female
Age at onset[a]	13 (6–33)
Age at first examination	40 (23–47)
Disease duration at first examination[a]	13 (9–25)
SPRS[a]	22 (12–29)
Harding classification	26 pure / 8 complicated
Ocular/oculomotor abnormalities	Optic atrophy 1/34 (3%) Gaze evoked nystagmus 4/34 (12%) Saccadic pursuit 3/34 (9%)
Dysarthria/dysphagia	Pseudobulbar dysarthria 1/34 (3%) Dysphagia 1/34 (3%)
Ataxia	Upper limb ataxia 2/34 (6%) Lower limb/gait ataxia 16/34 (47%)
Spasticity	Upper limb 8/34 (24%) Lower limb32/34 (94%)
Weakness	Upper limb (reduced fine motor movements) 1/34 (3%) Lower limb 29/34 (85%) None (5/34 (15%)
Tendon reflexes	Upper limb increased 13/34 (38%) Lower limb increased 33/34 (97%)
Plantar response	Extensor 34/34 (100%)
Muscle atrophy	Intrinsic hand muscles 2/34 (6%)
Vibration sense	Decreased 30/32 (94%)
Joint position sense	Reduced 24/33 (73%)
Surface sensation	Upper limb reduced 1/34 (3%) Lower limb reduced 17/34 (50%) Normal 17/34 (50%)
Temperature discrimination	Lower limb reduced 9/28 (32%)
Bladder	Voiding and/or urge incontinence 18/33 (55%)
Rectum	Urge incontinence 5/33 (15%)
Others	Epilepsy, panic disorder, substance abuse, cluster headache, early ovarian failure, congenital hip dysplasia

[a]Median (IQR).

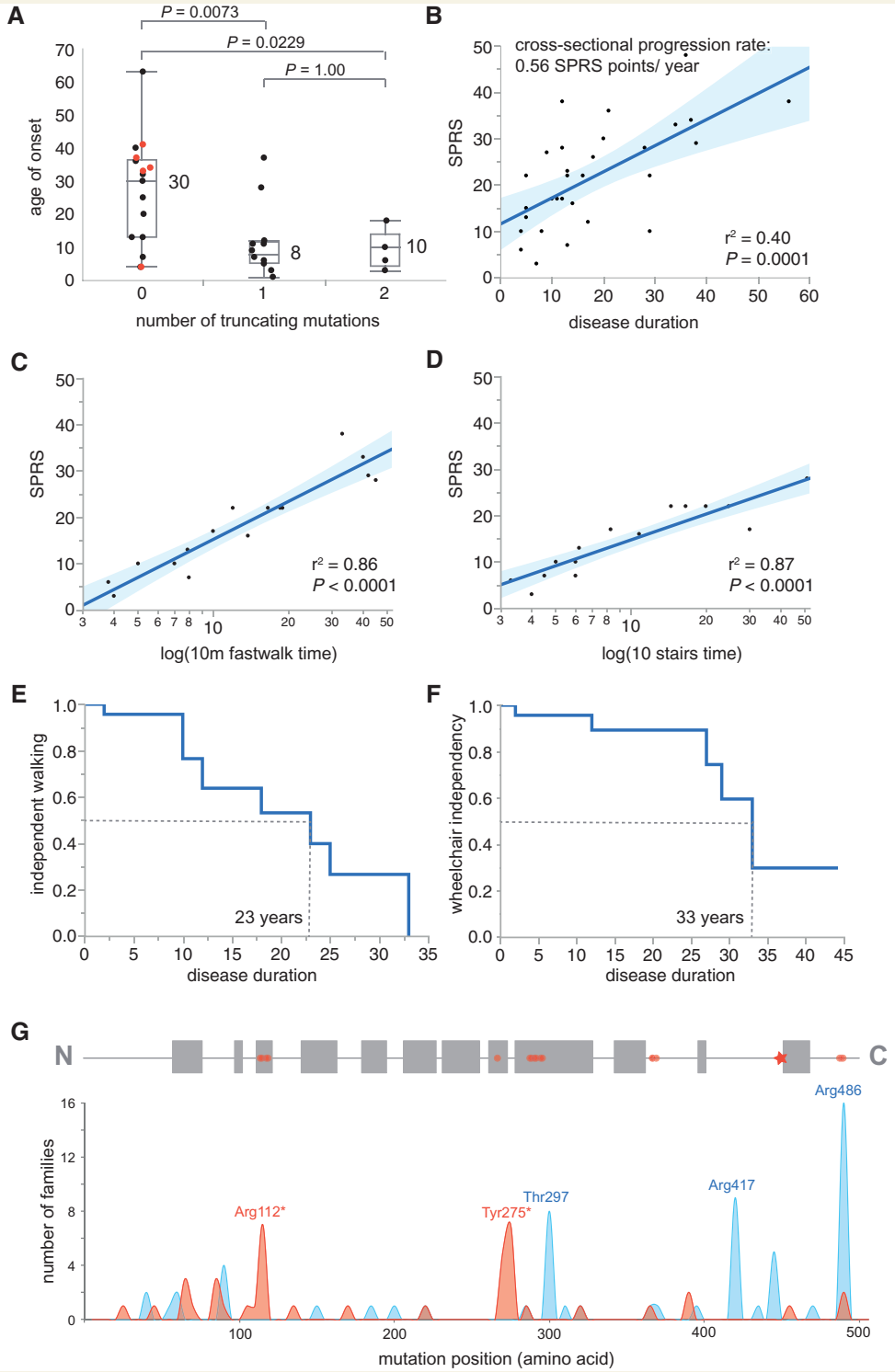

Figure 1 Cross-sectional and time-to-event analyses of disease severity and progression. (**A**) Age of onset distribution: patients with bi-allelic missense mutations had a later age of onset [median 30 years (IQR 13–37)] than those with either one [median 8 years (IQR 5–12)] or two [median 10 years (IQR 5–14)] truncating mutations (Mann-Whitney U-test, two-sided). The median age of onset in the total cohort was 13 years (IQR 6–32). Patients carrying the Arg486Cys mutation on both alleles are marked by red dots. With the exception of one case (Patient F10.1), all carriers of the homozygous Arg486Cys mutation manifested beyond the age of 30 years. Notably, all carriers of an Arg486Cys allele, which has a minor allele frequency of 0.1% in the European population while it is absent in the Latino population, were of European decent. (**B**) SPRS score by disease duration: disease severity as measured by the SPRS strongly correlated with disease duration in this cross-sectional cohort of SPG5 cases (n = 31). The fitted cross-sectional progression rate (SPRS points per year with the disease) is 0.56 points/year. The 95% confidence interval of the modelled fit is shaded in blue. (**C**) Fast walk (10 m) by SPRS: the time needed to cover a 10 m distance on a flat surface including one turn (item 3 of the SPRS) strongly correlated with the SPRS (n = 19). The best fit was reached after logarithmic transformation of

(continued)

of the SPRS total score (Fig. 1C and D). The logarithm of the 10 m fast walk time (item 3) and the time needed to climb 10 steps (item 5) explain 86% and 87% of the variability of the SPRS total score ($P < 0.0001$), respectively.

Longitudinal disease progression: SPRS

To determine longitudinal disease progression rates, we performed prospective follow-up examinations. A total of 65 SPRS examinations were available in 21 patients with a median follow-up interval of 12.4 months (IQR 8.1–24.3) and a median total follow-up time (first to last) of 31.0 months (IQR 15.0–53.8). To determine the prospective progression rate, we performed a linear mixed model with SPRS score as dependent variable and disease duration at examination as continuous covariate. This approach yielded a prospective progression rate of 0.80 SPRS points per year (95% CI 0.59–1.01, $P < 0.0001$; Fig. 2A).

Association of age of onset, disease duration, and genotype with disease severity

To determine which factors influence disease severity in SPG5 we performed a linear mixed model with the SPRS score as dependent and disease duration, age of onset, gender, and mutation type (truncating/missense) as independent variables.

No significant effects were observed for age of onset, gender or mutation type, neither when entered in the model alone [age of onset: unstandardized regression coefficient $B = -0.14$, 95% CI −0.63–0.35, $P = 0.56$; gender (female): $B = 4.24$, 95% CI −6.93–15.41, $P = 0.44$; mutation type (missense): $B = -9.55$, 95% CI −19.93–0.82, $P = 0.069$], nor when entered together with disease duration. However, for medium and long disease durations (medium and upper tertile of the disease duration spectrum) higher age of onset was associated with more severe disease (SPRS). This was not true for shorter disease durations (lower tertile of the disease duration spectrum; interaction $P = 0.013$; Fig. 2E–G). Disease duration was thus the most relevant predictor for disease severity, with additional predictive information contributed also by age of onset.

Serum and cerebrospinal fluid biomarkers

Oxysterol levels in serum and cerebrospinal fluid

25- and 27-OHC as well as 3β-CA are substrates for 7α-hydroxylase CYP7B1. We have previously shown in a small cohort of four SPG5 patients that mutations of *CYP7B1* lead to marked accumulation of oxysterols in serum and CSF (Schule *et al.*, 2010). We here found 25-OHC levels in serum to be elevated almost 90-fold compared to healthy controls and levels of 27-OHC and 3β-CA to be increased ∼6-fold each (Table 2). Levels of 24S-OHC, another side-chain-oxidized cholesterol metabolite that is not metabolized by CYP7B1, were unaltered.

In CSF of SPG5 patients, 27-OHC levels were increased ∼25-fold and 3β-CA was increased to ∼9-fold over normal levels while 24-OHC levels were unchanged (Table 2).

In heterozygous mutation carriers, a similar pattern was identified, albeit with less pronounced changes. 27-OHC was elevated 1.5-fold in serum and ∼5-fold in CSF and 25-OHC and 3β-CA were also moderately elevated (Table 2).

Correlation of oxysterols with disease severity

Next, we explored whether oxysterol levels in serum and CSF were correlated with clinical measures. Among all oxysterols tested (24-OHC, 25-OHC, 27-OHC, 3β-CA), only serum 27-OHC was found to be significantly associated with disease severity as measured by the SPRS score ($r^2 = 0.36$; $P = 0.007$; $n = 19$) (Fig. 2C). When testing for association with disease duration, again only serum 27-OHC was found to be significantly associated with disease duration ($r^2 = 0.33$; $P = 0.010$) after adjusting the significance level for multiple testing (Fig. 2D).

Pathophysiological relevance of oxysterols in SPG5

We investigated the effects of increasing concentrations of 24S-OHC, 25-OHC, 27-OHC and 3β-CA on viability and metabolic activity of motor neuron like cells (NSC-34) as well as cortical neurons derived from human iPSCs. In

Figure 1 Continued

the *x*-axis. This measure is valid only for patients that are still able to walk and was accordingly not applicable in three cases (Patients F1.1, F14.1 and F14.2). (**D**) Ten steps of stairs by SPRS: the time needed to navigate 10 steps including one turn with or without support of the banister (item 5 of the SPRS) strongly correlated with the SPRS ($n = 19$). The best fit was reached after logarithmic transformation of the *x*-axis. This measure was available only for cases still able to walk steps and therefore not applicable in three cases (Patients F1.1, F14.1 and F14.2). (**E**) Loss of independent ambulation: Kaplan-Meier analysis indicating the probability of SPG5 cases to become dependent on a walking aid (blue line). The median disease duration until SPG5 cases depend on a walking aid is 23 years ($n = 23$). (**F**) Wheelchair dependency: Kaplan-Meier analysis indicating the probability of SPG5 cases to become dependent on a wheelchair (blue line). The median disease duration until SPG5 cases depend on a wheelchair is 33 years ($n = 23$). (**G**) Mutation spectrum in SPG5. *Top:* Structure of the CYP7B1 protein: The *CYP7B1* gene encodes the 506 amino acid protein hydroxycholesterol 7-α-hydroxylase (NP_004811). Several alpha helices are predicted for CYP7B1 (Cui *et al.*, 2013) (marked by grey boxes). Predicted active site residues are labelled by red circles; the heme binding site (Cys449) is marked by an asterisk. *Bottom:* Frequency of mutations in SPG5. The histogram shows the frequency of published mutations including this study in SPG5 families. Truncating mutations (nonsense, frameshift, splice) are depicted in red, missense mutations and inframe insertions/deletions in blue. There are several mutational hotspots in SPG5; the amino acid residues most commonly affected by missense mutations are the active site residue Arg486 (16 families), Arg417 (nine families) and Thr297 (eight families).

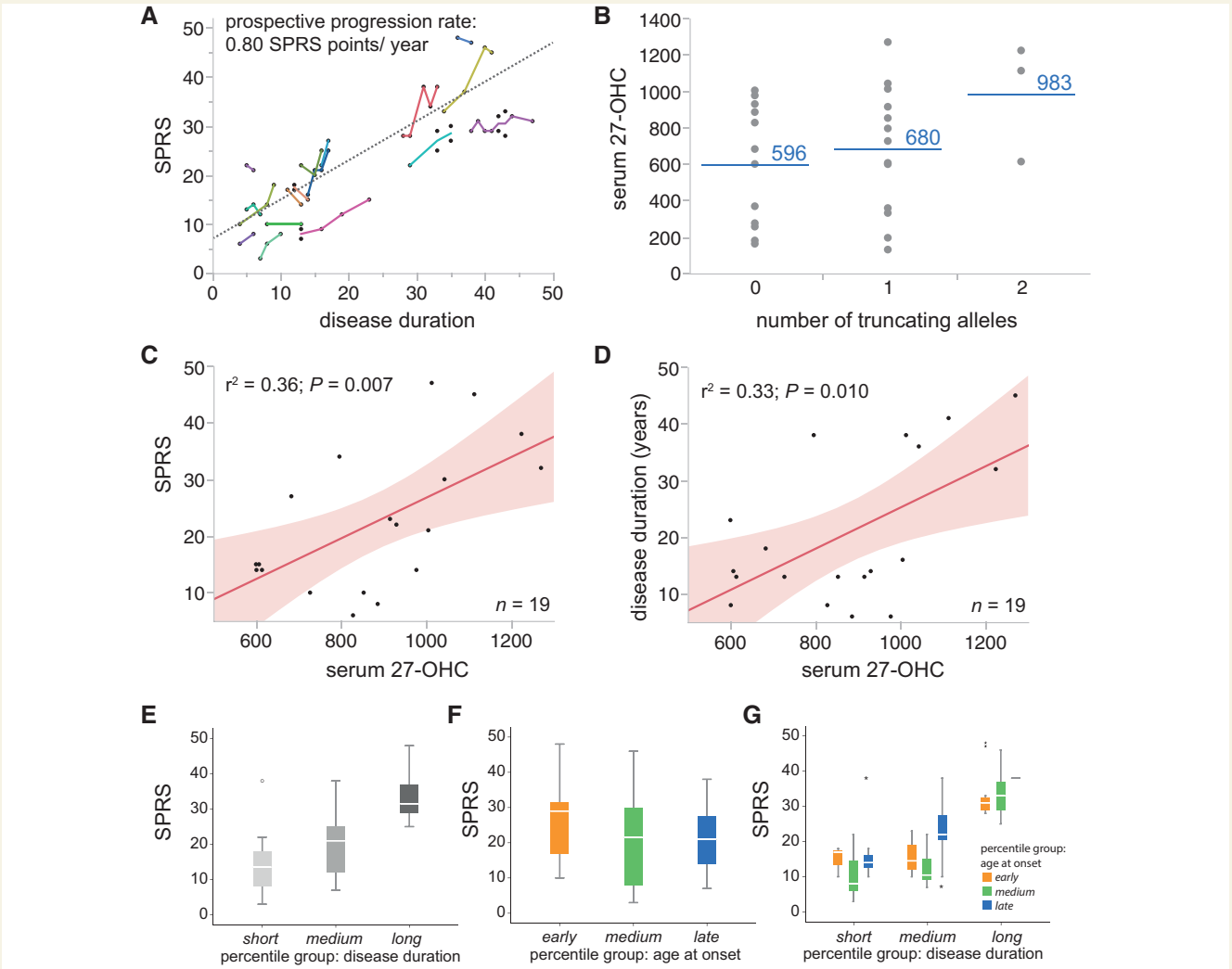

Figure 2 Longitudinal disease progression rate, factors influencing disease severity and oxysterol association with clinical parameters. (**A**) Longitudinal follow-up examinations in 21 SPG5 patients over a median follow-up interval of 12.4 months. The superimposed dotted grey line indicates the prospective progression rate of 0.80 SPRS points per year, derived from a linear mixed model with SPRS score as dependent variable and disease duration at examination as fixed effect. (**B**) Levels of 27-OHC (in serum) in dependence on the mutation type. Patients that carry missense mutations on both alleles have lower levels of 27-OHC in serum than cases with mono- or bi-allelic truncating mutations. Blue lines indicate median 27-OHC levels in serum. (**C** and **D**) Higher levels of 27-OHC in serum are associated with more severe disease and explain 36% of the variability of the SPRS score ($P = 0.007$). In cross-sectional data obtained from 19 SPG5 patients serum 27-OHC levels are furthermore higher at later disease stages ($r^2 = 0.33$; $P = 0.010$). (**E**) Disease severity increases with longer disease durations. Groups 'short', 'medium' and 'long' correspond to subgroups of the total cohort classified into tertiles ($n = 19$). (**F**) No differences of disease severity are observed depending on age of onset tertiles when considering the total cohort ($n = 19$). (**G**) In the subgroups with medium and long disease duration, later onset is associated with more severe disease ($n = 19$).

summary, all tested oxysterols interfere with metabolic activity and are cytotoxic at certain concentrations (Fig. 3). The relationship between oxysterol concentration and impact on metabolic activity and cell viability hereby appears to be linear. However, only 25-OHC and 27-OHC are harmful at concentrations comparable to levels measured in serum of SPG5 patients, whereas 3β-CA and 24-OHC exert their toxic effects only at considerably higher concentrations (3β-CA: ~60-fold patient levels; 24-OHC: ~35-fold patient levels). Hereby, cortical neurons surprisingly tolerated higher 27-OHC and 3β-CA concentrations than NSC-34 cells (Supplementary material).

Effects of oxysterol exposure on morphology

NSC-34 cells exposed to oxysterols (Supplementary Fig. 2) showed a significant reduction in total neurite length as well as branching points.

Randomized placebo-controlled clinical trial

As cholesterol and 27-OHC levels are closely related (Thelen *et al.*, 2006), we hypothesized that treatment of SPG5 patients with HMG-CoA reductase inhibitors can

Table 2 Oxysterol levels in SPG5 patients, heterozygous carriers and controls

	SPG5 patients	Heterozygous carriers	Controls
Serum	*n* = 19	*n* = 11	Dzeletovic *et al.* (1995); Norlin *et al.* (2000)
24-OHC (ng/ml)[a]	57.5 ± 9.2 (range 39–70)	59.4 ± 18.2 (range 31–88)	64 (range 30–127)
25-OHC (ng/ml)[a]	177.9 ± 77.0 (range 91–318)	15.4 ± 5.3 (range 8–26)	2 (range 0–11)
27-OHC (ng/ml)[a]	878.2 ± 207.1 (range 600–1270)	238.5 ± 83.4 (range 131–369)	154 (range 89–243)
3β-CA (ng/ml)[a]	363.1 ± 82.1 (range 226–514)	125.5 ± 50.1 (range 64–239)	59 SD 16
CSF	*n* = 17	*n* = 2[b]	
24-OHC (ng/ml)[a]	1.1 ± 0.4 (range 0.5–1.8)	2.0 (1.8 | 2.1)	1.4 (0.8–2.4)
27-OHC (ng/ml)[a]	12.9 ± 4.3 (range 6.5–25.2)	2.4 (1.9 | 2.9)	0.5 (0.5–0.8)
3β-CA (ng/ml)[a]	18.3 ± 5.7 (range 7.8–27.8)	2.1 (1.8 | 2.3)	<2 ng/ml

[a]Mean ± standard deviation (SD)
[b]Individual values are given in brackets.
25-OHC levels in CSF are close to the detection limit and are therefore not reported. N/A = not applicable.

lower the pathologically elevated levels of 25-OHC, 27-OHC, and 3β-CA. To test this hypothesis, we initiated a randomized placebo-controlled clinical trial (Statin Therapy of Oxysterol Pathology in SPG5; STOP-SPG5) with atorvastatin tested against placebo in a total of 14 SPG5 patients. No demographic differences were recognized between the verum and placebo groups at baseline (Supplementary Table 4). Atorvastatin was given at a dosage of 40 mg/day for 9 weeks in adults and 20 mg/day in children under 18 years of age.

Safety and tolerability

Atorvastatin was well tolerated, leading to a 0% drop-out rate. Compliance rate was high (mean 98%, minimum 89%) based on returned medication counts. A total of five adverse events were reported, including three in the placebo group ($n = 2$ post-dural-puncture headache; $n = 1$ stomach flu) and two in the verum group [$n = 1$ GGT elevation from 109 to 119 U/l (P10); $n = 1$ prolonged menstrual bleeding]. None of the adverse events was considered to be in causal relationship to the investigational drug. No serious adverse events were observed. Liver transaminase levels (AST, ALT, GGT) did not change significantly with treatment. Creatine kinase levels remained within normal limits in all probands before and after treatment (Supplementary Table 5).

Oxysterol response in serum and cerebrospinal fluid

Cholesterol in serum was lowered by 40% (range 35–48%) in the atorvastatin but not in the placebo group (two-sided $P < 0.001$, Mann-Whitney U-test; Table 3 and Fig. 4A). Atorvastatin also significantly reduced serum 27-OHC ($P = 0.001$) compared to placebo; the primary study endpoint was thus reached. Similarly, atorvastatin—but not placebo—reduced 24S-OHC ($P < 0.001$) and 25-OHC ($P = 0.002$) in serum. The effect was strongest for 27-OHC with a median reduction of 31.5% (range 16–42%) and could be demonstrated in every single proband of the atorvastatin group. In contrast, 3β-CA levels showed a rather large variability in the atorvastatin as well as the placebo group with reduction in some and increase of levels in other patients with no significant difference between groups (Table 3 and Fig. 4C).

In contrast, no significant difference in the changes of CSF levels of 24S-OHC, 27-OHC, or 3β-CA was observed with atorvastatin compared to placebo (Table 3 and Fig. 4D).

Effects on clinical outcome parameters

As expected in this short-term trial, no effects of atorvastatin were seen on clinical parameters either in the SPRS ($P = 0.735$) or in walking distance in the 3-min endurance walk ($P = 0.135$), or the physical cost index ($P = 0.530$) (Supplementary Table 6).

Discussion

SPG5 is an ultra-rare disease with an estimated prevalence of about 1:1 000 000 (Schule *et al.*, 2016) and a total number of 56 published families (Tsaousidou *et al.*, 2008; Biancheri *et al.*, 2009; Criscuolo *et al.*, 2009; Goizet *et al.*, 2009; Schule *et al.*, 2009; Cao *et al.*, 2011; Schlipf *et al.*, 2011; Arnoldi *et al.*, 2012; Noreau *et al.*, 2012; Kumar *et al.*, 2013; Roos *et al.*, 2013; Di Fabio *et al.*, 2014; Lan *et al.*, 2015). Multiple factors, including low public awareness for the disease, small numbers of patients available for clinical trials and limited market size, impede development of disease-specific therapies. However, an

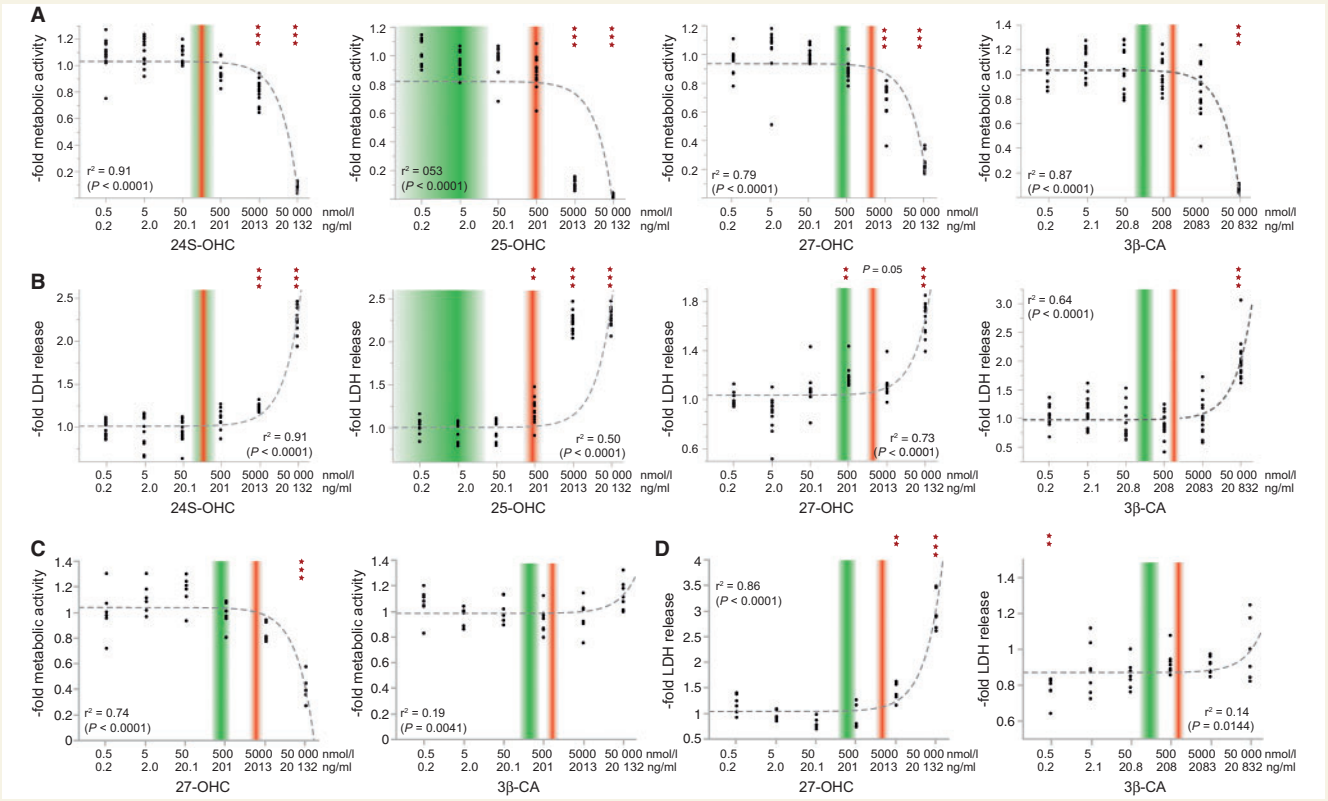

Figure 3 Neurotoxicity of oxysterols. The motor neuron-like cell line NSC-34 (**A** and **B**) as well as cortical neurons derived from iPSCs (**C** and **D**) were exposed to increasing concentrations of 24S-OHC, 25-OHC, 27-OHC and 3β-CA. (**A** and **C**) Metabolic activity was assessed by measuring the cleavage of the tetrazolium salt WST-1 in a colorimetric assay. (**B** and **D**) LDH-release in the medium was analysed as a measure of cytotoxicity. The range of oxysterol concentration in the serum of healthy controls is indicated by shaded green boxes. Shaded red boxes show the range of values observed in SPG5 patients. Dotted grey lines are fitted following a linear regression model. The horizontal axis is log-scaled.

improved understanding of the pathogenesis following the discovery of the commonly monogenetic aetiology work to the advantage of orphan diseases and sometimes allow 'personalized' treatment approaches with registered drugs or well characterized compounds. SPG5 is an ideal candidate for such an approach as CYP7B1 deficiency affects the well-studied and druggable bile acid synthesis pathway.

Phenotype and disease progression

Here, we report on a cohort of 34 patients from 28 families. SPG5 typically manifests within the first two decades of life. The majority of carriers of missense mutations on both alleles however typically manifest in adulthood (Fig. 1A). This phenomenon might be explained by higher residual enzymatic activity of CYP7B1, leading to lower levels of 27-OHC in serum (Fig. 2B). The clinical phenotype of SPG5 is characterized by slowly progressive spastic paraplegia accompanied by rather severe dorsal column sensory deficits manifesting as gait ataxia that exceeds the degree of sensory deficits commonly seen in HSP (Schule *et al.*, 2016). Although the SPG5 phenotype is rather homogenous, there is considerable overlap with other pure or oligosystemic forms of HSP, hampering phenotype-based genotype prediction on a single case basis.

SPG5 progresses with a rate of 0.56 SPRS points per year in our cross-sectional cohort; this progression rate is slightly lower than the longitudinal progression rate of 0.8 SPRS points per year obtained in a smaller subcohort of 21 SPG5 cases. As the cross-sectional progression rate relies on the self-reported age of symptom onset, the longitudinal progression rate is more likely to reflect the true progression of SPG. Walking aid dependency occurred after a median of 23 years in SPG5; in this respect SPG5 therefore behaves almost identically to HSP in general (median 22 years in Schule *et al.*, 2016). The median duration until wheelchair dependency however was 33 years in SPG5; in a general HSP cohort, only a quarter of patients became wheelchair-dependent in a comparable timeframe (first quartile 37 years in Schule *et al.*, 2016). SPG5 patients may therefore be more likely than other HSP patients to become wheelchair-dependent.

Oxysterols are valuable biomarkers in SPG5

The mechanism of action for all mutations tested so far appears to be loss of oxysterol-7α-hydroxylase enzymatic function. This was demonstrated by an elevation of the

Table 3 Oxysterol and cholesterol levels before and after treatment

Variable	Verum				Placebo				Verum versus Placebo
	Before	After	Median change	Median change %	Before	After	Median change	Median change %	P-value*
Cholesterol (s)	172 (146–251)	103 (93–135)	−69 (−107 – −52)	−40.1% (−42.9 – −34.9)	163 (151–184)	152 (136–193)	−11 (−15–11)	−6.7% (−8.2–5.2)	< 0.001
LDL	108 (87–167)	42 (40–59)	−63 (−108 – −45)	−56.3% (−63.0 – −53.3)	101 (84–104)	94 (72–124)	−7 (−11–6)	−6.9% (−11.2–4.5)	< 0.001
HDL	51 (41–84)	49 (40–66)	−3 (−18 – −1)	−5.0% (−20.4 – −2.4)	51 (47–70)	55 (45–71)	−3 (−6–5)	−4.1% (−11.8–7.1)	0.476
Triglycerides	80 (54–107)	48 (38–78)	−23 (−29 – −6)	−27.1% (−36.1 – −13.6)	88 (53–100)	67 (63–95)	+ 2 (−32–14)	+ 4.7% (−26.4–26.4)	0.200
24S-OHC (S)	60 (54–67)	46 (38–54)	−14 (−16 – −10)	−25.8% (−29.6 – −15.0)	51 (42–57)	52 (43–56)	+ 1.0 (−1–1)	+ 1.6% (−1.8–2.4)	< 0.001
25-OHC (S)	158 (105–251)	118 (85–190)	−40 (−61 – −11)	−22.7% (−25.3 – −10.9)	120 (91–170)	120 (86–177)	−5.0 (−9–7)	−4.2% (−7.0–5.4)	0.002
27-OHC (S)	853 (683–1113)	641 (507–694)	−307 (−409 – −144)	−31.5% (−37.8 – −20.4)	727 (600–886)	740 (587–848)	−1 (−27–40)	−0.12% (−4.4–4.1)	0.001 (one-sided)
3β-CA (S)	427 (271–513)	387 (363–536)	+ 42 (−12–69)	+ 8.2% (−5.2–18.3)	374 (285–425)	357 (301–474)	−15 (−23–49)	−4.5% (−6.1–11.5)	0.318
24S-OHC (CSF)	1.0 (1.0–1.8)	1.0 (0.8–1.8)	0.0 (−0.2–0)	0.0% (−20.0–0)	1.2 (1.0–1.6)	1.0 (1.0–1.6)	0.0 (−0.2–0.1)	0.0% (−16.7–11.1)	0.694
27-OHC (CSF)	14.1 (6.8–14.9)	13.1 (6.1–14.3)	−0.7 (−1.2–0)	−8.4% (−10.8–0)	11.7 (10.4–15.8)	10.4 (9–14.8)	−1.0 (−1.2 – −0.2)	−6.7% (−10.3 – −1.2)	1.000
3β-CA (CSF)	17.7 (10.5–22.6)	22.4 (12.6–25.9)	+ 2.0 (−1.3–2.9)	+ 9.4% (−7.3–37.2)	17.8 (16.2–24.5)	17.3 (13.6–22.5)	0.0 (4.2–0.6)	0.0% (−23.6–3.7)	0.402

*Exact Mann-Whitney U-test, two-sided.
Values are median (IQR) in ng/ml.
Verum group: $n = 7$; Placebo group: $n = 7$. S = serum; LDL = low density lipoprotein; HDL = high density lipoprotein.

substrates of oxysterol-7α-hydroxylase (25-OHC, 27-OHC and 3β-CA) in serum and CSF of SPG5 patients while levels of 24S-OHC, product of the hydroxylation of cholesterol by *CYP46A1*, were normal. Our data thus confirm previous observations in smaller cohorts of up to four SPG5 cases (Schule *et al.*, 2010; Theofilopoulos *et al.*, 2014). The accumulation of these three substrates was not only observable as a group effect, but also true for each single SPG5 patient included in this study. The range of values thereby did not show any overlap between SPG5 patients and heterozygous mutation carriers or controls. Both serum and CSF levels of 25-OHC, 27-OHC and 3β-CA are therefore potentially useful diagnostic biomarkers in SPG5 and can be used to validate missense variants of unknown significance in CYP7B1.

In addition to the diagnostic potential of measuring oxysterol concentrations in SPG5, these metabolites may have pathogenetic relevance. In support of this hypothesis we demonstrate that 27-OHC impairs metabolic activity and viability of a spinal cord like motor neuron cell line (NSC-34) and iPSC-derived cortical neurons (Fig. 3) at concentrations close to those measured in serum of SPG5 patients. No comparable effect of 3β-CA was observed. Moreover, 27-OHC (in serum) levels, but not levels of the other oxysterols measured in this study, increased over the course of the disease and are correlated with disease severity (Fig. 2C and D). Taken together, these results indicate that among the deregulated oxysterols observed in SPG5, the elevated 27-OHC levels may have a particular relevance in terms of pathogenesis and disease course. It has previously been demonstrated that 3β-CA exerts toxic effects on rodent oculomotor neurons *in vitro* and zebrafish motor neurons *in vivo* via activation of neuronal LRX receptors (Theofilopoulos *et al.*, 2014). Although we cannot disprove the pathogenic relevance of this metabolite in SPG5, the missing correlation of 3β-CA levels with disease duration or disease severity do not support this hypothesis.

STOP-SPG5: a randomized controlled trial targeting oxysterol pathology in SPG5

The potential pathogenetic relevance of 27-OHC and/or other oxysterols in SPG5 offers a chance for a disease-modifying therapy. Concentrations of oxysterols are considerably higher in serum than in the CNS. As oxysterols are able to pass the blood–brain barrier there is a net flux of 27-OHC and most probably also 25-OHC from the circulation to the brain (Leoni *et al.*, 2003; Heverin *et al.*, 2005). The CNS is the main site where pathology occurs in SPG5; therefore, this influx of oxysterols from the circulation into the CNS is likely to be a key contributor to SPG5 pathogenesis. As cholesterol and 27-OHC levels in the circulation are closely correlated (Babiker *et al.*, 2005) we have suggested earlier that SPG5 patients may benefit from a cholesterol lowering therapy, which may in turn

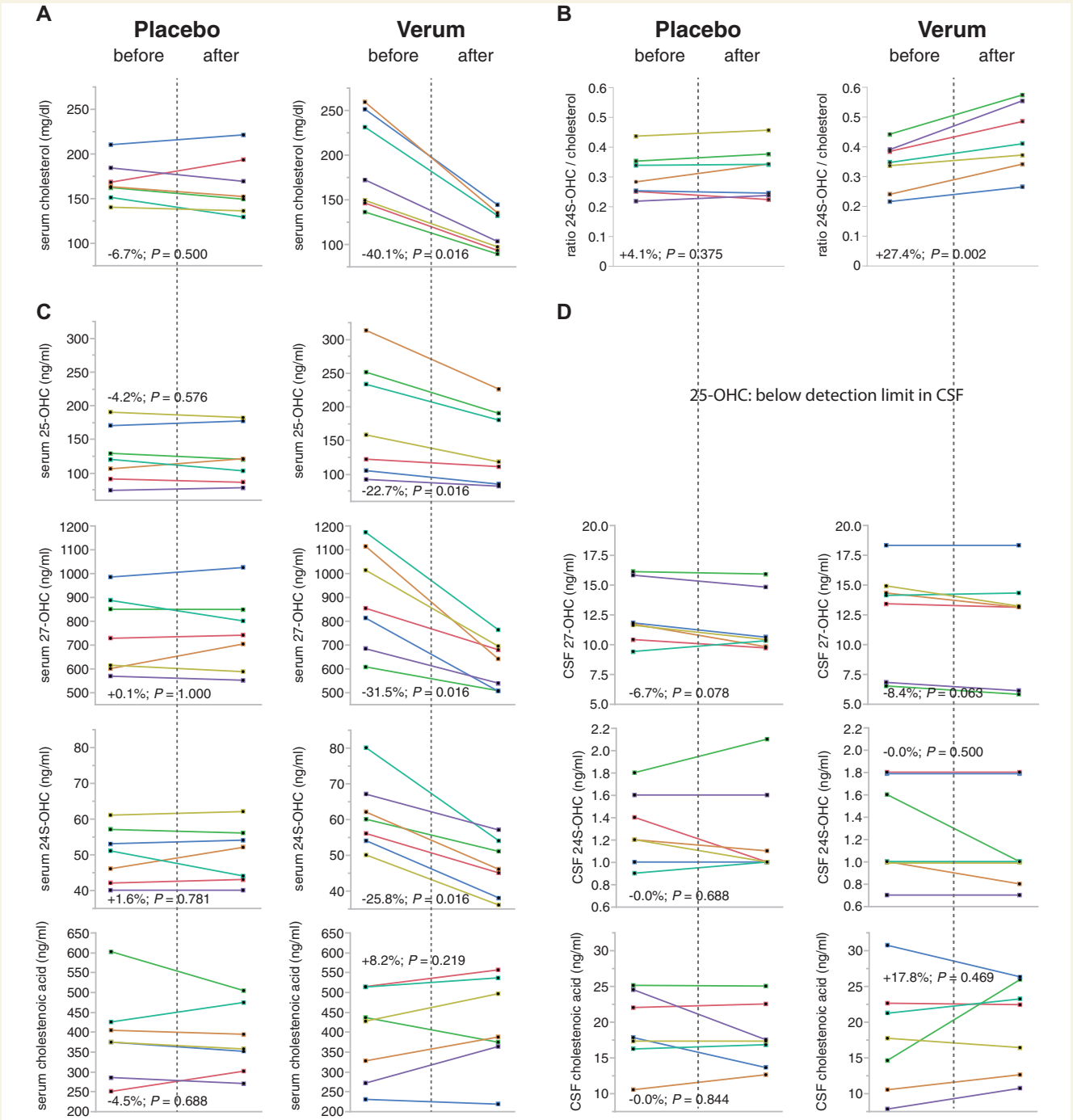

Figure 4 Individual treatment responses. Individual levels of cholesterol and oxysterols before and after treatment with placebo (*left* column) or atorvastatin (*right* column). Data from serum analyses are given in (**A** and **C**) and for CSF in **D**. The mean change of values across the group and the *P*-value for a sign rank test is given for each analyte. The ratio between brain-derived 24S-OHC and cholesterol (**B**) can be used as an indirect indicator of station effects on brain cholesterol metabolism (Thelen *et al.*, 2006).

also lower elevated oxysterol levels (Schule *et al.*, 2010). Following up on this concept, Mignarri *et al.* (2015) reported a decrease of 27-OHC (in serum) levels by up to 55% after variable treatment regimens with cholesterol-lowering drugs in single patients. Systematic studies of this effect in a controlled trial setting, however, were missing. Moreover, it had not been demonstrated whether the decrease of 27-OHC in serum translates into the CSF compartment. We therefore performed a randomized, double-blind, placebo-controlled trial and administered the cholesterol-lowering drug atorvastatin or placebo to SPG5 patients. Serum 27-OHC reduction was selected as

primary outcome as (i) we have demonstrated 27-OHC neurotoxicity on patient-derived cortical neurons when added to the culture medium at concentrations similar to those found in serum of SPG5 patients (Fig. 3); and (ii) serum 27-OHC correlates with disease duration and severity (Fig. 2C and D). Our study demonstrates that 9 weeks of atorvastatin treatment indeed leads to a significant reduction of 27-OHC levels in serum by 31.5%. Additionally, both 24S-OHC and 25-OHC were reduced by atorvastatin treatment, not 3β-CA, however, a downstream metabolite of 27-OHC. The most likely explanation for this observation is that low cholesterol levels favour the production of 3β-CA from 27-OHC (Pikuleva *et al.*, 1998), thus shifting the 3β-CA /27-OHC balance towards 3β-CA.

Despite this clear treatment effect, the moderate dose of atorvastatin we chose for this trial (40/20 mg) only partially normalized oxysterol levels in SPG5. 27-OHC levels after treatment (median 641 ng/ml) were still higher than levels measured in healthy heterozygous carriers of CYP7B1 mutations (median 239 ng/ml; Table 2). The threshold levels of oxysterols that lead to neurotoxicity after long-term exposure are unknown other than that the elevated levels observed in heterozygous carriers seem to be tolerated in the long run. Increase of the atorvastatin dose alone most likely won't lead to a substantially higher treatment effect as increase of atorvastatin from 40 mg to 80 mg is expected to add only another 5% to the cholesterol lowering effect (Silva *et al.*, 2007; Nicholls *et al.*, 2010) and may have even less effect in normolipidaemic subjects (Cilla *et al.*, 1996; Millar *et al.*, 2010). Combination of a statin with ezetimibe, which inhibits cholesterol resorption, however, might lead to a more pronounced treatment effect. Indeed, a 55% reduction of serum 27-OHC was demonstrated in a single case treated with simvastatin and ezetimibe combination therapy over a 12-month period (Mignarri *et al.*, 2015).

Under physiological conditions, most of the 27-OHC present in CSF originates from the circulation (Leoni *et al.*, 2003). Serum levels of 27-OHC are ~300-fold higher than CSF levels (~150 ng/ml in serum versus ~0.5 ng/ml in CSF) (Meaney *et al.*, 2001); diffusion is the most likely driving force for the influx of 27-OHC into the CSF. We thus expected atorvastatin to affect CSF oxysterol levels to a similar extent as serum levels. We were, however, surprised to find no significant effect of atorvastatin on CSF metabolites compared to placebo. The well-established relation between plasma cholesterol and brain oxysterol levels (Leoni *et al.*, 2003; Heverin *et al.*, 2005) as well as the relation between plasma and CSF levels of 27-OHC (Leoni *et al.*, 2003) appear to be abrogated in SPG5. This could be explained by (i) a reduced permeability of the blood–brain barrier in SPG5 patients. Normal serum/CSF albumin ratios before as well as after treatment, however, suggest integrity of the blood–brain barrier also in SPG5 patients; (ii) an increased half-life of 27-OHC in the CNS due to the genetic CYP7B1 deficiency. Other than the liver, in which 27-OHC can alternatively be metabolized by other enzymes, e.g. the cholesterol-7-α-hydroxylase (CYP7A1) (Norlin *et al.*, 2000), the brain likely relies heavily on CYP7B1 function to metabolize 27-OHC (Fig. 5). In fact, the efficient turnover of 27-OHC in brain under physiological conditions with a half-life of less than an hour may be the true 'driving force' behind the net flux of 27-OHC from the circulation to the brain. It is well documented that the levels of CYP7B1 in the brain are unusually high in relation to other organs (Stapleton *et al.*, 1995). In SPG5, CYP7B1 metabolism therefore may be more compromised in brain compared to the periphery, leading to over-proportional accumulation of 27-OHC and other oxysterols in CSF compared to the serum compartment (~30-fold increase in the CSF compared to ~6-fold increase in serum; Table 2); (iii) *in situ* production of 27-OHC in the brain may contribute more than previously thought to the total pool of 27-OHC in the CNS. The brain contains some sterol 27-hydroxylase (CYP27A1) (Meaney *et al.*, 2007) and thus has the capacity to convert cholesterol into 27-OHC. The ratio between the brain-derived cholesterol metabolite 24S-OHC and serum cholesterol increased with atorvastatin treatment in the verum group (Fig. 4B) (Thelen *et al.*, 2006), thus indicating that brain cholesterol may be less affected by atorvastatin treatment than serum cholesterol. This may limit the effect of atorvastatin treatment on *in situ* production of 27-OHC in the brain.

Additionally, the clinical effect of statin treatment remains to be shown. Given the slowly progressive nature of the disease, long-term follow-up of SPG5 patients on statin treatment is required. This is now on the way in our cohort and will help to decide whether the promising effect of atorvastatin on oxysterols in serum translates into a positive influence on the disease course in SPG5 patients.

In conclusion, this study demonstrates:

(i) Side-chain oxidized oxysterols and 3β-CA are consistently elevated in serum and CSF of SPG5 patients and can thus be used to validate the pathogenicity of variants of unknown significance in CYP7B1. Moreover, higher levels of 27-OHC are associated with longer disease durations and more severe disease.

(ii) Side-chain oxidized oxysterols like 24-OHC, 25-OHC and 27-OHC are toxic in neuronal cell cultures. 27-OHC especially appears to be deleterious in concentrations close to those found in SPG5 patients. This supports a key pathogenic role for 27-OHC in SPG5 and puts forth 27-OHC as a biomarker in interventional trials.

(iii) Short-term treatment with atorvastatin significantly lowers the levels of the toxic metabolite 27-OHC in serum of SPG5 patients (primary endpoint) and therefore provides proof-of-principle for a first causal treatment strategy in SPG5.

(iv) Genetic stratification allowed us to conduct this sufficiently powered randomized controlled clinical trial with only seven cases per treatment arm, thus

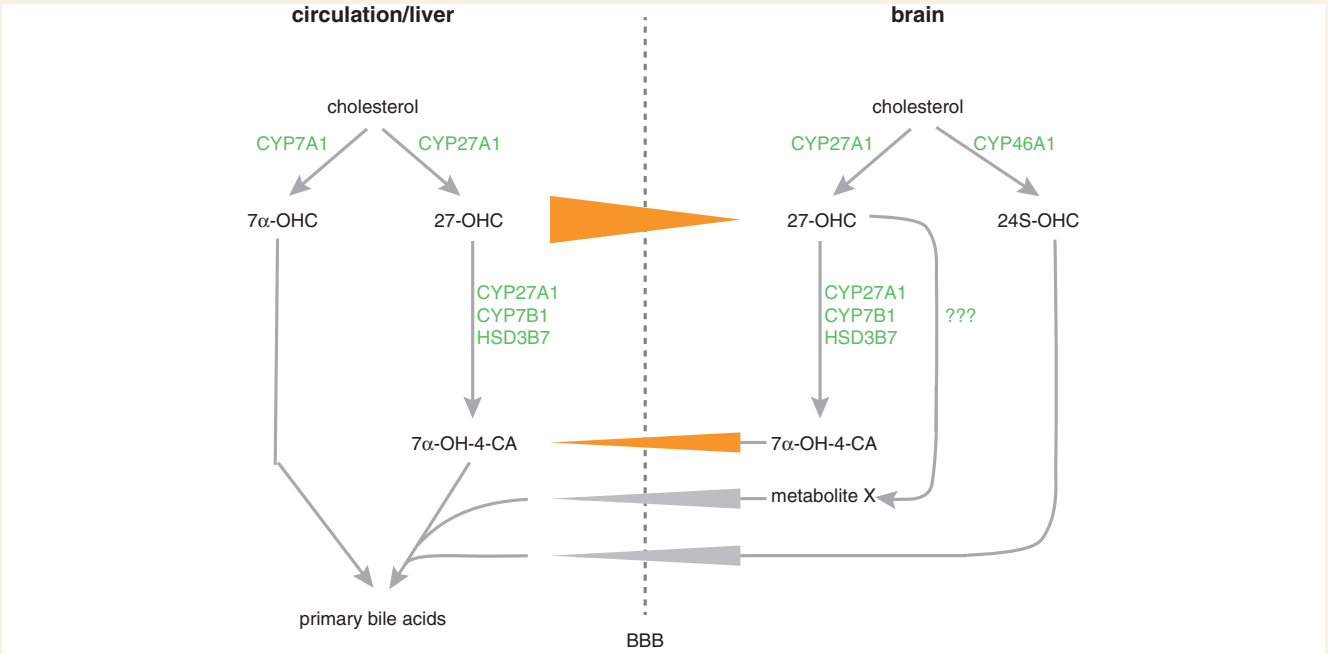

Figure 5 Oxysterol flux across the blood–brain barrier. 27-OHC is produced both in the periphery and the CNS by 27α-hydroxylation of cholesterol. A net flux of 27-OHC from the circulation to the CNS has been demonstrated (Heverin *et al.*, 2005), that is most likely driven by the concentration gradient between blood and CSF (~150 ng/ml 27-OHC in serum versus ~0.5 ng/ml 27-OHC in CSF). To eliminate 27-OHC from the CNS, it is metabolized to 7α-hydroxy-3-oxo-4-cholestenoic acid (7α-OH-4-CA), requiring the action of three key enzymes: sterol 27-hydroxylase (CYP27A1), oxysterol 7α-hydroxylase (CYP7B1), and 3β-hydroxy-C27-steroid dehydrogenase/isomerase (HSD3B7). 7α-OH-4-CA is transferred efficiently across the blood–brain barrier (Meaney *et al.*, 2007). However, the flux of 7α-OH-4-CA from the brain is too low as to fully explain the elimination of 27-OHC from the CNS (Meaney *et al.*, 2007). Further routes to metabolize and excrete 27-OHC to the circulation therefore have to be assumed (see 'metabolite X' in the figure). BBB = blood–brain barrier.

leveraging the advantage of monogenetic diseases over more common neurodegenerative disorders that often comprise pathophysiologically heterogeneous groups of patients.

(v) Due to the presumed long half-life of 27-OHC in CSF of SPG5 patients, longer treatment durations will be necessary until the serum reduction of 27-OHC translates to a concomitant reduction of 27-OHC in the CSF compartment. The well-established relation between plasma cholesterol and brain oxysterol levels under physiological conditions needs to be reconsidered in SPG5.

(vi) The short-term reduction of 27-OHC in serum by ~31% appears not to be sufficient to correct accumulation of 27-OHC in the CSF. A more marked reduction of 27-OHC in the circulation will likely be necessary to reverse the concentration gradient between circulation and the CNS.

(vii) Our study clearly shows the importance to measuring CSF in addition to serum levels of oxysterols in interventional trials of SPG5 in the future.

Before atorvastatin can be recommended for the treatment of SPG5 patients, longitudinal data should be awaited to prove sustained tolerance of the drug and favourable long-term effects on oxysterol levels in CSF.

Acknowledgements

The skilful support of Jutta Eymann, Elke Feil, Jennifer Reichbauer, Yvonne Theurer, Avencia Sanchez-Mejias and Stefanie Weißenberger in many practical aspects of this study is gratefully acknowledged. We also thank Constanze Gallenmüller and Clemens Küpper for assistance with patient recruitment and care. We thank our patients and their families for participation. Without their readiness to travel often long distances this trial would not have been possible.

Funding

This study was supported by the European Union within the 7th European Community Framework Program through funding for the NEUROMICS network (F5-2012-305121 to L.S., P.B., J.B. and P.D.J.), the E-Rare Network NEUROLIPID (01GM1408B to R.S. and M.T.B.) and a Marie Curie International Outgoing Fellowship (grant PIOF-GA-2012-326681 to R.S. and L.S.). Further support was provided by the US National Institutes of Health (NIH) (grants R01NS075764 and U54NS065712 to S.Z:, grant 5R01NS072248 to R.S. and S.Z., grant U54NS092091 to R.S. and S.Z.), the

Association Belge contre les Maladies Neuromusculaire (ABMM) - Aide à la Recherche ASBL, the Ministerium für Wissenschaft, Forschung und Kunst Baden-Württemberg and the Europäischen Sozialfonds in Baden-Württemberg (grant to S.W.), the Eva-Luise and Horst Köhler foundation (grant to R.S.), the German HSP-Selbsthilfegruppe e.V. (grant to R.S. and L.S.), Swedish Brain Power, Hjärnfonden and the Stockholm County (grants to I.B.), the Italian Ministry of Health (grant RC1016001 to A.M.) and the Brazilian funding agencies MCTI/CNPQ/Universal 14/2014 (460941/2014-3) and FIPE-HCPA (GPPG-HCPA 14-0695). T.R. is supported by the Clinician Scientist Program of the University of Tübingen (#386-0) and J.B. is supported by a Senior Clinical Researcher mandate of the Research Fund - Flanders (FWO).

Supplementary material

Supplementary material is available at *Brain* online.

References

Arnoldi A, Crimella C, Tenderini E, Martinuzzi A, D'Angelo MG, Musumeci O, et al. Clinical phenotype variability in patients with hereditary spastic paraplegia type 5 associated with CYP7B1 mutations. Clin Genet 2012; 81: 150–7.

Babiker A, Dzeletovic S, Wiklund B, Pettersson N, Salonen J, Nyyssonen K, et al. Patients with atherosclerosis may have increased circulating levels of 27-hydroxycholesterol and cholestenoic acid. Scand J Clin Lab Invest 2005; 65: 365–75.

Biancheri R, Ciccolella M, Rossi A, Tessa A, Cassandrini D, Minetti C, et al. White matter lesions in spastic paraplegia with mutations in SPG5/CYP7B1. Neuromuscul Disord 2009; 19: 62–5.

Bjorkhem I, Falk O. Assay of the major bile acids in serum by isotope dilution-mass spectrometry. Scand J Clin Lab Invest 1983; 43: 163–70.

Bjorkhem I, Leoni V, Meaney S. Genetic connections between neurological disorders and cholesterol metabolism. J Lipid Res 2010; 51: 2489–503.

Borg G. ATS statement: guidelines for the six-minute walk test (vol 166, pg 111, 2002). Am J Respir Crit Care Med 2016; 193: 1185.

Cao L, Fei QZ, Tang WG, Liu JR, Zheng L, Xiao Q, et al. Novel mutations in the CYP7B1 gene cause hereditary spastic paraplegia. Movement disorders : official journal of the Movement Disorder Society 2011; 26: 1354–6.

Cilla DD, Jr., Gibson DM, Whitfield LR, Sedman AJ. Pharmacodynamic effects and pharmacokinetics of atorvastatin after administration to normocholesterolemic subjects in the morning and evening. J Clin Pharmacol 1996; 36: 604–9.

Crapo RO, Casaburi R, Coates AL, Enright PL, MacIntyre NR, McKay RT, et al. ATS statement: Guidelines for the six-minute walk test. American Journal of Respiratory and Critical Care Medicine 2002; 166: 111–7.

Criscuolo C, Filla A, Coppola G, Rinaldi C, Carbone R, Pinto S, et al. Two novel CYP7B1 mutations in Italian families with SPG5: a clinical and genetic study. J Neurol 2009; 256: 1252–7.

Cui YL, Zhang JL, Zheng QC, Niu RJ, Xu Y, Zhang HX, et al. Structural and dynamic basis of human cytochrome P450 7B1: a survey of substrate selectivity and major active site access channels. Chemistry 2013; 19: 549–57.

Di Fabio R, Marcotulli C, Tessa A, Leonardi L, Storti E, Pierelli F, et al. Sensory ataxia as a prominent clinical presentation in three families with mutations in CYP7B1. J Neurol 2014; 261: 747–51.

Dzeletovic S, Breuer O, Lund E, Diczfalusy U. Determination of cholesterol oxidation products in human plasma by isotope dilution-mass spectrometry. Anal Biochem 1995; 225: 73–80.

Famer D, Meaney S, Mousavi M, Nordberg A, Bjorkhem I, Crisby M. Regulation of alpha- and beta-secretase activity by oxysterols: cerebrosterol stimulates processing of APP via the alpha-secretase pathway. Biochem Biophys Res Commun 2007; 359: 46–50.

Goizet C, Boukhris A, Durr A, Beetz C, Truchetto J, Tesson C, et al. CYP7B1 mutations in pure and complex forms of hereditary spastic paraplegia type 5. Brain 2009; 132(Pt 6): 1589–600.

Harding AE. Classification of the hereditary ataxias and paraplegias. Lancet 1983; 1: 1151–5.

Hauser S, Hoflinger P, Theurer Y, Rattay TW, Bjorkhem I, Schule R, et al. Stem cell-based disease modeling of hereditary spastic paraplegia type 5. Human gene therapy 2016; 27: A76–7.

Heverin M, Meaney S, Lutjohann D, Diczfalusy U, Wahren J, Bjorkhem I. Crossing the barrier: net flux of 27-hydroxycholesterol into the human brain. J Lipid Res 2005; 46: 1047–52.

Iriberri M, Galdiz JB, Gorostiza A, Ansola P, Jaca C. Comparison of the distances covered during 3 and 6 min walking test. Respir Med 2002; 96: 812–6.

Kumar KR, Blair NF, Vandebona H, Liang C, Ng K, Sharpe DM, et al. Targeted next generation sequencing in SPAST-negative hereditary spastic paraplegia. J Neurol 2013; 260: 2516–22.

Lan MY, Yeh TH, Chang YY, Kuo HC, Sun HS, Lai SC, et al. Clinical and genetic analysis of Taiwanese patients with hereditary spastic paraplegia type 5. Eur J Neurol 2015; 22: 211–4.

Leoni V, Masterman T, Patel P, Meaney S, Diczfalusy U, Bjorkhem I. Side chain oxidized oxysterols in cerebrospinal fluid and the integrity of blood-brain and blood-cerebrospinal fluid barriers. J Lipid Res 2003; 44: 793–9.

Lim WL, Martins IJ, Martins RN. The involvement of lipids in Alzheimer's disease. Journal of genetics and genomics = Yi chuan xue bao 2014; 41: 261–74.

MacGregor J. The evaluation of patient performance using long-term ambulatory monitoring technique in the domiciliary environment. Physiotherapy 1981; 67: 30–3.

Meaney S, Hassan M, Sakinis A, Lutjohann D, von Bergmann K, Wennmalm A, et al. Evidence that the major oxysterols in human circulation originate from distinct pools of cholesterol: a stable isotope study. J Lipid Res 2001; 42: 70–8.

Meaney S, Heverin M, Panzenboeck U, Ekstrom L, Axelsson M, Andersson U, et al. Novel route for elimination of brain oxysterols across the blood-brain barrier: conversion into 7alpha-hydroxy-3-oxo-4-cholestenoic acid. J Lipid Res 2007; 48: 944–51.

Mignarri A, Malandrini A, Del Puppo M, Magni A, Monti L, Ginanneschi F, et al. Treatment of SPG5 with cholesterol-lowering drugs. J Neurol 2015; 262: 2783–5.

Millar JS, Ky B, Wolfe ML, Pruscino L, Baer A, Rader DJ. Short-term treatment with high-dose atorvastatin reduces LDL cholesterol but shows no anti-inflammatory effects in normolipidemic subjects with normal CRP levels. Clin Transl Sci 2010; 3: 140–6.

Nicholls SJ, Brandrup-Wognsen G, Palmer M, Barter PJ. Meta-analysis of comparative efficacy of increasing dose of Atorvastatin versus Rosuvastatin versus Simvastatin on lowering levels of atherogenic lipids (from VOYAGER). Am J Cardiol 2010; 105: 69–76.

Noreau A, Dion PA, Szuto A, Levert A, Thibodeau P, Brais B, et al. CYP7B1 mutations in French-Canadian hereditary spastic paraplegia subjects. Can J Neurol Sci 2012; 39: 91–4.

Norlin M, Andersson U, Bjorkhem I, Wikvall K. Oxysterol 7 alpha-hydroxylase activity by cholesterol 7 alpha-hydroxylase (CYP7A). J Biol Chem 2000; 275: 34046–53.

Pikuleva IA, Babiker A, Waterman MR, Bjorkhem I. Activities of recombinant human cytochrome P450c27 (CYP27) which produce

intermediates of alternative bile acid biosynthetic pathways. J Biol Chem 1998; 273: 18153–60.

Prasanthi JR, Huls A, Thomasson S, Thompson A, Schommer E, Ghribi O. Differential effects of 24-hydroxycholesterol and 27-hydroxycholesterol on beta-amyloid precursor protein levels and processing in human neuroblastoma SH-SY5Y cells. Mol Neurodegener 2009; 4: 1.

Rantham Prabhakara JP, Feist G, Thomasson S, Thompson A, Schommer E, Ghribi O. Differential effects of 24-hydroxycholesterol and 27-hydroxycholesterol on tyrosine hydroxylase and alpha-synuclein in human neuroblastoma SH-SY5Y cells. J Neurochem 2008; 107: 1722–9.

Riendeau V, Garenc C. Effect of 27-hydroxycholesterol on survival and death of human macrophages and vascular smooth muscle cells. Free Radic Res 2009; 43: 1019–28.

Roos P, Svenstrup K, Danielsen ER, Thomsen C, Nielsen JE. CYP7B1: novel mutations and magnetic resonance spectroscopy abnormalities in hereditary spastic paraplegia type 5A. Acta Neurol Scand 2013.

Schlipf NA, Schule R, Klimpe S, Karle KN, Synofzik M, Schicks J, et al. Amplicon-based high-throughput pooled sequencing identifies mutations in CYP7B1 and SPG7 in sporadic spastic paraplegia patients. Clin Genet 2011; 80: 148–60.

Schule R, Brandt E, Karle KN, Tsaousidou M, Klebe S, Klimpe S, et al. Analysis of CYP7B1 in non-consanguineous cases of hereditary spastic paraplegia. Neurogenetics 2009; 10: 97–104.

Schule R, Holland-Letz T, Klimpe S, Kassubek J, Klopstock T, Mall V, et al. The Spastic Paraplegia Rating Scale (SPRS): a reliable and valid measure of disease severity. Neurology 2006; 67: 430–4.

Schule R, Siddique T, Deng HX, Yang Y, Donkervoort S, Hansson M, et al. Marked accumulation of 27-hydroxycholesterol in SPG5 patients with hereditary spastic paresis. J Lipid Res 2010; 51: 819–23.

Schule R, Wiethoff S, Martus P, Karle KN, Otto S, Klebe S, et al. Hereditary spastic paraplegia: Clinicogenetic lessons from 608 patients. Ann Neurol 2016; 79: 646–58.

Shi Y, Kirwan P, Livesey FJ. Directed differentiation of human pluripotent stem cells to cerebral cortex neurons and neural networks. Nat Protoc 2012; 7: 1836–46.

Silva M, Matthews ML, Jarvis C, Nolan NM, Belliveau P, Malloy M, et al. Meta-analysis of drug-induced adverse events associated with intensive-dose statin therapy. Clin Ther 2007; 29: 253–60.

Stapleton G, Steel M, Richardson M, Mason JO, Rose KA, Morris RG, et al. A novel cytochrome P450 expressed primarily in brain. J Biol Chem 1995; 270: 29739–45.

Thelen KM, Laaksonen R, Paiva H, Lehtimaki T, Lutjohann D. High-dose statin treatment does not alter plasma marker for brain cholesterol metabolism in patients with moderately elevated plasma cholesterol levels. J Clin Pharmacol 2006; 46: 812–6.

Theofilopoulos S, Griffiths WJ, Crick PJ, Yang S, Meljon A, Ogundare M, et al. Cholestenoic acids regulate motor neuron survival via liver X receptors. J Clin Invest 2014; 124: 4829–42.

Tsaousidou MK, Ouahchi K, Warner TT, Yang Y, Simpson MA, Laing NG, et al. Sequence alterations within CYP7B1 implicate defective cholesterol homeostasis in motor-neuron degeneration. Am J Hum Genet 2008; 82: 510–5.